Fullerene Synthesis

DOI: 10.1002/anie.201006588

Template-Assisted Formation of Fullerenes from Short-Chain Hydrocarbons by Supported Platinum Nanoparticles**

Francesc Viñes and Andreas Görling*

Since the discovery of C_{60} fullerenes,[1] research on the respective family of carbon allotropes has grown enormously,[2] mainly motivated by potential technological applications. Fullerenes are of interest in molecular electronics and for nonlinear optical devices.[3] Metal–insulator transitions of alkali-intercalated fullerenes[4] and superconductivity of alkali-doped fullerene compounds have attracted considerable scientific attention;[5] the great interest in fullerene-based materials has boosted the search for a rational design of fullerenes by new synthesis strategies.[6]

Fullerenes usually are obtained by vaporization methods,[6] but can also be synthesized from polyarene precursor $C_{60}H_{30}$ (**1**). Scott and co-workers have reported fullerene formation in the gas phase either through a series of cyclodehydrogenation steps[7] on **1** or through cyclization of a trichloroderivative, $C_{60}H_{27}Cl_3$.[6,8] These methods, however, lead to yields below 1%. Recently, Otero and co-workers showed that a Pt(111) single crystal surface-mediated process can achieve almost a 100% yield,[9,10] using **1** and the precursor $C_{60}H_{27}N_3$ (**2**) to eventually obtain, after annealing over 750 K, fullerene and triazafullerene species. Nevertheless, the yield for the synthesis of the precursors from commercial chemicals is still only 33% for **1** and 56% for **2**.

The great improvement of the latter studies is to employ organic compounds, whose inherent geometric structure (exhibiting several interconnected C_6 and C_5 rings) and electronic structure (strong aromaticity) favor the formation of fullerenes. Inspired by this idea the following question arises: Is it possible to synthesize fullerenes from simple and abundant precursors with the help of templates, whose specific geometric and electronic structures enable a natural formation of fullerenes? This means that the formation of fullerenes is induced by specific properties of a template which acts, in addition, as a catalyst during the synthesis process. In the ideal case, the use of pertinent templates would favor the formation of specific fullerenes and, by mixing small heteroatom-containing molecules with the precursors, of heterofullerenes.

Herein we show the possibility of using supported nanoparticles as templates and catalysts for the fullerene synthesis from simple precursor molecules, considering as a proof of principle, the synthesis of a simple fullerene, C_{60}, from methane or ethylene by nanometer-sized platinum nanoparticles on an oxide support. By means of state-of-the-art ab initio calculations based on DFT we give arguments for the effectiveness of this set-up. For a successful fullerene synthesis sketched here, several conditions have to be fulfilled: 1) the precursor molecules have to be completely dehydrogenated at the Pt nanoparticles, releasing the hydrogen atoms as gaseous hydrogen (H_2(g)) at working temperature, 2) C atoms or intermediate carbon compounds have to remain at the Pt nanoparticle and must not migrate to the support, and 3) the formation of fullerenes must be energetically more favorable than that of other carbon allotropes, in particular graphene structures (sheet-like carbon phases). Below we show how all three criteria can be met.

As a catalyst, we propose nanometer-sized Pt particles that expose (111) facets of a certain size corresponding to a C_{60} diameter $\varnothing$. Particles with at least one (111) facet that contains 12 close-packed Pt atoms have a diameter of approximately 0.72 nm, which is similar to the fullerene diameter calculated herein as $\varnothing = 0.71$ nm. Figure 1 a,b depicts examples of two possible nanoparticles with a cut cuboctahedral structure, which is typical for face-centered-cubic (fcc) metal nanoparticles. Larger versions of such nanoparticles have been observed by STM for Pd supported on Al_2O_3.[11] Theoretical basin-hopping global optimizations predict similar structures for various noble metals of up to 200

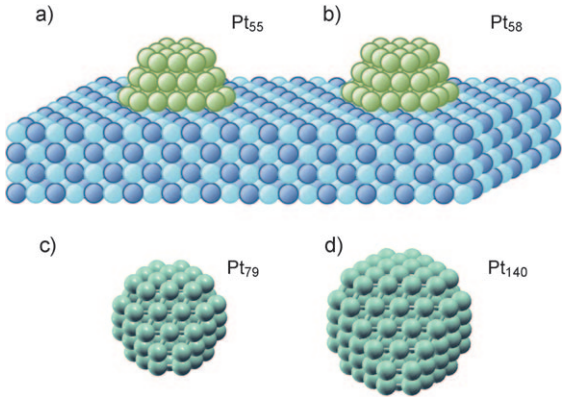

Figure 1. Sketches of subnanometer particles of a) Pt_{55} and b) Pt_{58} supported by an oxide film and structures of c) Pt_{79} and d) Pt_{140} nanoparticles used in the calculations.

[*] Dr. F. Viñes, Prof. Dr. A. Görling
Friedrich-Alexander-Universität Erlangen-Nürnberg
Lehrstuhl für Theoretische Chemie and Interdisciplinary Center for Interface Controlled Processes
Egerlandstrasse 3, 91058 Erlangen (Germany)
E-mail: francesc.vines@chemie.uni-erlangen.de

[**] F.V. thanks the Alexander von Humboldt-Foundation for his postdoctoral grant. Funding of the German Research Council (DFG) in the Cluster of Excellence "Engineering of Advanced Materials" (www.eam.uni-erlangen.de) at the University of Erlangen-Nuremberg is gratefully acknowledged.

Supporting information for this article is available on the WWW under http://dx.doi.org/10.1002/anie.201006588.

atoms on MgO(001) surfaces.[12] Recently, Vajda et al.[13] have developed the soft-landing method, which allows the deposition of subnanometer Pt particles on MgO thin films with a size precision of ± 1 atom. All these experimental advances in controlling clusters sizes and theoretical predictions on shapes demonstrate that supported nanoparticles that resemble those depicted in Figure 1 a,b can indeed be formed.

As a source of carbon atoms here, we consider ethylene and methane. Ethylene is a convenient source of carbon atoms on Pt(111) single crystals because of its high sticking coefficient and because it completely dehydrogenates at temperatures above 400 K.[14] Methane is quite economic due to its natural abundance; however, it has a very low sticking coefficient. Nevertheless, molecular beam (MB) experiments[15,16] showed that nanometer-sized Pt nanoparticles can completely dehydrogenate methane at temperatures between 460–500 K by recombining the hydrogen atoms and releasing them as H_2(g). Recent MB experiments combined with DFT calculations[17] showed that energy barriers drop substantially when methane dehydrogenates at the edges and corners of Pt nanoparticles, which is caused by the higher activity of the low-coordination sites and their flexibility in the accommodation of adsorbed species. As a result, a complete methane dehydrogenation can occur at such Pt nanoparticles at temperatures as low as 100 K. In summary, a complete dehydrogenation of methane or ethylene at Pt nanoparticles is feasible and, thus, criterion (1) of the above list seems to have been met. For the formation of heterofullerenes, heteroatom-containing precursors must dehydrogenate likewise. Recent studies showed that species such as ammonia (NH_3) and sulfur hydride (H_2S) dehydrogenate at temperatures below 450 K.[18,19]

With respect to the support, the simplest case would be a material that plays no active role. Hence, C atoms should be catalytically generated at the Pt nanoparticles, should stay on those particles, and eventually cluster to form fullerene-like composites. C atoms that for some reason would be present on the support should be thermodynamically driven to the Pt nanoparticles, which would act as a hub of carbon atoms. Present DFT calculations of C atom adsorption and diffusion on slab models of different supports show that carbide substrates (TiC) would be inappropriate, since the adsorption energy of single C atom species on them is 8 kJ mol^{-1} larger than on Pt(111) surfaces (see Table 1), which serve as a reference for Pt nanoparticles.[20] This observation points to an easy diffusion of carbon atoms to the carbide support and to remote zones of TiC, thus enabling the eventual formation of graphene at high C atom concentrations.

Table 1: Adsorption energies (E_{ads}) of isolated carbon atoms.[a]

	Al_2O_3(001)	MgO(001)	BaO(001)	TiC(001)	Pt(111)
E_{ads} [kJ mol^{-1}]	239	146	390	574	566
site[b]	T^O	T^O	T^O	H^{TiTiC}	H^f

[a] At $\Theta = 0.5$ ML on the most stable adsorption sites of (001) surfaces of different oxides and TiC, and on the Pt(111) surface. [b] T or H specify adsorption on an on-top or three-fold hollow site. Indices at sites indicate which surface atoms the carbon atom is bonded to. *f* denotes adsorption on an fcc three-fold hollow site.

Reducible oxides such as CeO_2 or TiO_2 may release oxygen atoms that eventually migrate to Pt nanoparticles and recombine with C atoms to form CO or CO_2,[21] thus decimating the number of C atoms on the Pt nanoparticles. However, basic (MgO, BaO) and inert (Al_2O_3) oxides seem to meet the requirements of a low enough interaction with carbon atoms, indicating that a migration of carbon atoms to zones far from a Pt particle is thermodynamically very unlikely. Thus, for oxide surfaces such as MgO, BaO, or Al_2O_3 criterion (2) of the above list seems to be obeyed.

Finally, the crucial step of C_{60} formation from C atoms adsorbed on Pt nanoparticles, criterion (3) of the above list, shall be considered. For a first insight into the thermodynamic conditions, cohesive energies (E_{coh}) of free, that is, unsupported finite graphene-like structures are compared to the E_{coh} of graphene and C_{60} fullerene in Figure 2. It is shown that the cohesive energy of graphene fragments is highly dependent on their size. Gas-phase C_{60} species are thermodynamically more stable than any isolated graphene flake with less than about 200 atoms, corresponding to a diameter of approximately 2.8 nm. Of course, the effect of the substrate, that is, the Pt nanoparticle, might modify this size limit.

The carbonaceous species C_1 and C_2 obtained after complete dehydrogenation of methane or ethylene exhibit a negative charge caused by a charge transfer from the Pt substrate.[20] This charge transfer gives rise to a mutual repulsion among species that hinders their eventual aggregation and thus the formation of larger aggregates. Present calculations show that the energy barrier of the formation of carbon dimers on extended Pt(111) surfaces at $\Theta = 0.5$ ML,

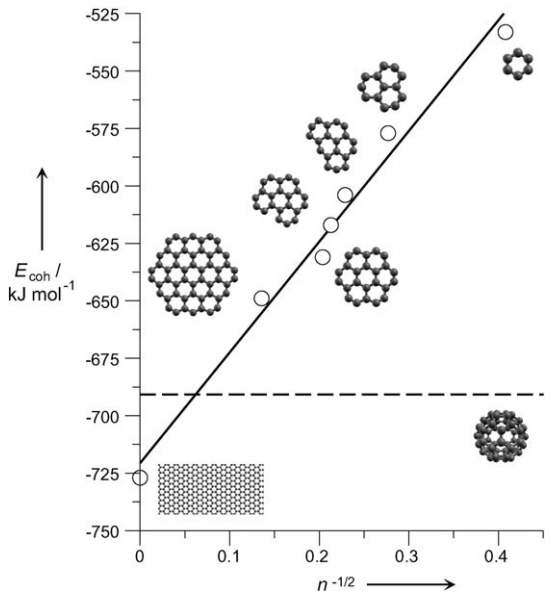

Figure 2. Linear behavior of the cohesive energy of graphene flakes of increasing size up to the infinite size limit. Cohesive energies per C atom (E_{coh}) are plotted against the linear dimension of the graphene flake represented as $n^{-1/2}$, where *n* is the number of carbon atoms. The dependence is strongly linear as shown by the regression coefficient *R* ($E_{coh} = -720.71 + 480.87\,n^{-1/2}$; $R = 0.992$). The dashed horizontal line illustrates the cohesive energy of fullerene C_{60}. Small gray spheres correspond to C atoms.

92 kJ mol^{-1}, is not negligible. However, such an energy barrier is still comparable to dehydrogenation barrier heights, hence suggesting clustering at dehydrogenation temperatures.[17] A merging of C_2 fragments to form C_4 species exhibits a much lower energy barrier of 35 kJ mol^{-1}. Indeed, the bigger the formed fragments are, the lower is the charge on them.[20] On extended surfaces, this leads to the adhesion of further carbon atoms to initial aggregates to finally form graphene. Graphene has been proven to incorporate further carbon atoms barrier-free on other transition-metal surfaces.[22] In this case, the clustering process would be diffusion-governed (at coverage $\Theta = 0.5$ ML it exhibits calculated energy barriers of 87 and 28 kJ mol^{-1} for C_1 and C_2 species, respectively). Previous DFT calculations[20] and experiments[23] show that the diffusion of carbon atoms on Pt(111) surfaces occurs at temperatures of 460–480 K. On Pt nanoparticles, diffusion of C atoms may occur at lower temperatures, according to present diffusion barrier estimates, which at particle edges are in the range of 20–70 kJ mol^{-1} for C_2 species, present calculations estimate a much lower diffusion temperature of 156 K. In summary, the formation of large carbonaceous aggregates on Pt nanoparticles can be expected to happen at reasonable temperatures and coverages.

To study whether the formation of fullerenes can occur on Pt nanoparticles, various structures and carbon patterns have been computationally optimized on a Pt_{79} nanoparticle, including situations with disperse carbon atoms, with graphene-like, and with fullerene-like structures; the results are summarized in Figure 3. At low coverage (number n of carbon atoms per Pt nanoparticle smaller than 13), arrangements in which the carbon atoms are completely dispersed over the particle facets are clearly preferred, in agreement with previous results on Pt(111) slabs.[20] For example, a dehydrogenated benzene C_6 ring on the center site of a (111)Pt_{79} facet is approximately 40 kJ mol^{-1} less stable than 6 C atoms, each located on the central site of one (111) facet.

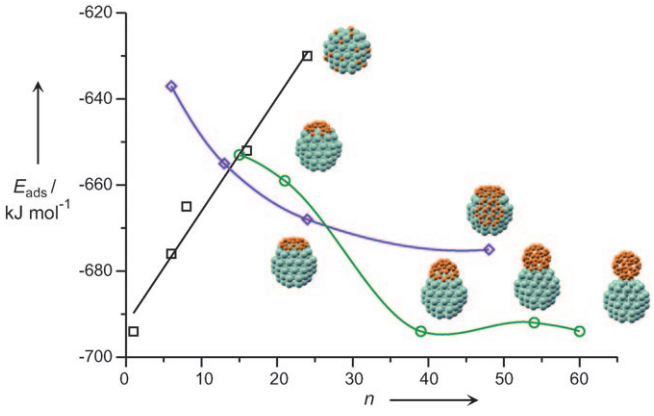

Figure 3. Evolution of different carbonaceous structures with number n of carbon atoms on a Pt_{79} nanoparticle. Shown are adsorption energies E_{ads} per C atom. For a given number n, the adsorption energies per C atom multiplied by n correspond to relative total energies. □: completely dispersed carbon atoms, ◇: hexagonal graphene-like structures on facets, and ○: fullerene-like structures on a given facet. Images depict the corresponding structures. Small orange and large light green spheres correspond to C and Pt atoms, respectively.

However, the stability of dispersed carbon patterns decreases rapidly with an increasing number of carbon atoms, thus favoring the formation of aggregated species. Compare for instance the situation with 24 C atoms dispersed over (111) facets, which is approximately 40 kJ mol^{-1} per carbon atom less stable than the graphene-like dehydrogenated coronene C_{24} molecule on a (111) facet. This means that at a high enough concentration of carbon atoms the formation of aggregates is thermodynamically favored on Pt nanoparticles.

For $13 < n < 24$, graphene-like structures seem to be preferred, although fullerene-like structures are close in energy. However, if more carbon atoms are provided to the particle, the situation is reversed. For instance, once C_{24} is formed on one facet, a further aggregation of graphene-like structures would lead to structures expanded over adjacent facets. This observation is illustrated with the "clap" arrangement that contains 48 C atoms, that is, two assembled C_{24} structures over adjacent Pt_{79}(111) facets. Such a structure is 7 kJ mol^{-1} more stable per C atom than two nonconnected C_{24} structures. However, fullerene-like structures like C_{39} or C_{54} are more stable by approximately 20 kJ mol^{-1} per C atom than the clap arrangement. Thus, Figure 3 clearly shows that if more than approximately 30 C atoms are present, they thermodynamically prefer to adopt fullerene-like structures on one facet rather than forming graphene-like sheets that cover more than one facet. Such great stability of intermediate species during C_{60} formation results mainly from the strong bonds between boundary atoms of fullerene intermediates and Pt atoms at edge and corner sites of the nanoparticle facet, which are formed because of the special activity and flexibility of edge and corner sites.

An alternative to the formation of fullerenes could be the formation of nanotube structures. Indeed, Schneider and coworkers reported the formation of single-walled carbon nanotubes on Ni from amorphous carbon produced from dehydrogenated ethylene.[24] However, present calculations of a capped single-walled C_{57} nanotube structure attached to the nanoparticle show that it is approximately 75 kJ mol^{-1} less stable than similar fullerene-like structures. Further tests on the bigger particle Pt_{140} ($\varnothing = 0.94$ nm) show that such preference for fullerene-like structures is kept. This result demonstrates that the C_{60} species would still be thermodynamically favored, even when using bigger nanoparticles, thus indicating that there may exist a broad range of Pt nanoparticles that can prompt fullerene formation. The nature of the process, the sequential incorporation of additional carbon atoms into a growing structure, may lead to fullerenes like C_{60}, even if for large numbers of carbon atoms (hundreds or thousands), carbon nanotubes are thermodynamically favored; if C_{60} is formed, though, the growth process might be interrupted and C_{60} may be generated as a kinetically stable product. Here the specific conditions of the growth process (concentration of C adatoms, size and shape of the Pt nanoparticles etc.) may control which fullerene, C_{60}, C_{70}, etc. is formed and whether carbon nanotubes are produced.

The present finding that all required conditions seem to be met strongly suggests the usage of Pt nanoparticle templates for the synthesis of fullerene structures. We believe that the versatility of the set-up (variations of size, geometry, chemical

nature of the nanoparticles and the support, changing composition and/or mixture of the precursors) may enable a tailor-made synthesis of fullerene-like structures, including heterofullerenes and endohedral fullerenes, which may be formed if traces of other species are dehydrogenated or present at the Pt nanoparticles together with the precursors.

Computational Methods

The DFT calculations were performed with the VASP code.[25] Interactions of valence electrons with the atomic cores were described by the projector-augmented plane-wave method.[26] Basis sets with kinetic energy of plane waves up to 415 eV were employed. Geometry optimizations were carried out using a conjugate gradient algorithm that ensures forces acting on each atom to be less than 0.03 kJ mol^{-1} pm^{-1}. The revised form of Perdew–Burke–Erzenhof[27] (revPBE) exchange-correlation functional has been used throughout the study. Previous studies showed that this functional gives accurate results for the adsorption of carbonaceous and other species.[17,20]

Large-scale, systematic, and accurate DFT investigations of the structure and reactivity of noble-metal nanoparticles with close to hundred atoms together with a full treatment of the substrate are computationally prohibitively expensive; because of this, all calculations that concern carbonaceous species on metal nanoparticles have been carried out on isolated cuboctahedral Pt_{79} and Pt_{140} nanoparticles (see Figure 1 c,d). These isolated nanocrystallites have proven in past studies to be representative of supported metal nanoparticles, thus providing an accurate description of chemical processes on them.[28–30]

Calculations on the (001) surfaces of MgO, BaO, and TiC required 4-layered slabs with a vacuum space of 0.1 nm. For Al_2O_3, a 6-layered slab (here, one layer consists of three sublayers in the form of Al-O_3-Al) was used. A Monkhorst-Pack mesh grid with at least $13\times13\times1$ k-point sampling was used for every support. In all slab models, the bottom-half layers have been fixed to their bulk revPBE optimal positions during structure optimization procedures (a_{MgO} = 423.4 pm; a_{BaO} = 563.0 pm; a_{TiC} = 434.6 nm; $a_{Al_2O_3}$ =479.8 pm, $c_{Al_2O_3}$ =1310.3 pm), while the other half layers and the adsorbates were fully relaxed. Further computational details of Pt(111) slabs and Pt nanoparticle models can be found elsewhere.[21]

Diffusion and aggregation transition states have been located employing the Climbing-Image Nudged-Elastic-Band method followed by a refinement with a Quasi-Newton method until forces acting on atoms are smaller than 0.03 kJ mol^{-1} pm^{-1}. Transition states have been characterized as saddle points of the potential energy hypersurface by examining the vibrational frequencies determined with a standard finite displacement method of 5 pm. Details of the estimation of diffusion temperatures have been described in previous work.[20]

Adsorption energies per carbon atom, E_{ads}, are obtained by subtraction of the energy of the complete arrangement of the substrate plus the adsorbed carbon species that contains a number n of C atoms from the sum of the energies of the relaxed bare substrate and n isolated C atoms and by subsequently dividing the energy difference by n. Cohesive energies of gas phase carbonaceous structures, E_{coh}, are obtained similarly by subtracting the energy of the carbon-based structure that contains n atoms from the sum of n isolated C atoms and by dividing the final energy by n. The energy of an isolated carbon atom is obtained with a spinpolarized calculation of one atom placed in the middle of a broken symmetry unit cell with the dimensions $0.9\times1.0\times1.1$ nm. Unless stated otherwise, the rest of the calculations were non-spinpolarized.

Received: October 20, 2010
Revised: March 1, 2011
Published online: April 14, 2011

Keywords: dehydrogenation · density functional calculations · fullerenes · nanostructured templates · platinum nanoparticles

[1] H. W. Kroto, J. R. Health, S. C. O'Brien, R. F. Curl, R. E. Smalley, *Nature* **1985**, *318*, 162 – 163.
[2] E. Osawa, *Perspectives in Fullerene Nanotechnology*, Kluwer, Dordrecht, **2002**.
[3] M. C. Petty, *Molecular Electronics*, Wiley-Interscience, Chichester, **2007**.
[4] R. C. Haddon, A. F. Hebard, M. J. Rosseinsky, D. W. Murphy, S. J. Duclos, K. B. Lyons, B. Miller, J. M. Rosamilia, R. M. Fleming, A. R. Kortan, S. H. Glarum, A. V. Makhija, A. J. Muller, R. H. Eick, S. M. Zahurak, R. Tycko, G. Dabbagh, F. A. Thiel, *Nature* **1991**, *350*, 320 – 322.
[5] K. Tanigaki, T. W. Ebbesen, S. Saito, J. Mizuki, J. S. Tsai, Y. Kubo, S. Kuroshima, *Nature* **1991**, *352*, 222 – 223.
[6] L. T. Scott, *Angew. Chem.* **2004**, *116*, 5102 – 5116; *Angew. Chem. Int. Ed.* **2004**, *43*, 4994 – 5007.
[7] M. M. Boorum, Y. V. Vasil′ev, T. Drewello, L. T. Scott, *Science* **2001**, *294*, 828 – 831.
[8] L. T. Scott, M. M. Boorum, B. J. McMahon, S. Hagen, J. Mack, J. Blank, H. Wegner, A. de Meijere, *Science* **2002**, *295*, 1500 – 1503.
[9] G. Otero, G. Biddau, C. Sánchez-Sánchez, R. Caillard, M. F. López, C. Rogero, F. J. Palomares, N. Cabello, M. A. Basanta, J. Ortega, J. Méndez, A. M. Echavarren, R. Pérez, B. Gómez-Lor, J. A. Martí-Gago, *Nature* **2008**, *454*, 865 – 868.
[10] L. T. Scott, *Angew. Chem.* **2009**, *121*, 444 – 445; *Angew. Chem. Int. Ed.* **2009**, *48*, 436 – 437.
[11] F. Viñes, A. Desikusumastuti, T. Staudt, A. Görling, J. Libuda, K. M. Neyman, *J. Phys. Chem. C* **2008**, *112*, 16539 – 16549.
[12] J. Goniakowski, A. Jelea, C. Mottet, G. Barcaro, A. Fortunelli, Z. Kuntová, F. Nitta, A. C. Levi, G. Rossi, R. Ferrando, *J. Chem. Phys.* **2009**, *130*, 174703.
[13] S. Vajda, M. J. Pellin, J. P. Greeley, C. L. Marshall, L. A. Curtiss, G. A. Ballentine, J. W. Elam, S. Catillon-Mucherie, P. C. Redfern, F. Mehmood, P. Zapol, *Nat. Mater.* **2009**, *8*, 213 – 216.
[14] J. R. Creighton, J. M. White, *Surf. Sci.* **1983**, *129*, 327 – 335.
[15] C. Papp, B. Tränkenschuh, R. Streber, T. Fuhrmann, R. Denecke, H.-P. Steinrück, *J. Phys. Chem. C* **2007**, *111*, 2177 – 2184.
[16] T. Fuhrmann, M. Kinne, B. Tränkenschuh, C. Papp, J. F. Zhu, R. Denecke, H.-P. Steinrück, *New J. Phys.* **2005**, *7*, 107.
[17] F. Viñes, Y. Lykhach, T. Staudt, M. P. A. Lorenz, C. Papp, H.-P. Steinrück, J. Libuda, K. M. Neyman, A. Görling, *Chem. Eur. J.* **2010**, *16*, 6530 – 6539.
[18] G. Novell-Leruth, A. Valcárcel, J. Pérez-Ramírez, J. M. Ricart, *J. Phys. Chem. C* **2007**, *111*, 860 – 868.
[19] D. R. Alfonso, *Surf. Sci.* **2008**, *602*, 2758 – 2768.
[20] F. Viñes, K. M. Neyman, A. Görling, *J. Phys. Chem. A* **2009**, *113*, 11963 – 11973.
[21] Y. Lykhach, T. Staudt, M. P. A. Lorenz, R. Streber, A. Bayer, H.-P. Steinrück, J. Libuda, *ChemPhysChem* **2010**, *11*, 1496 – 1504.
[22] S. Hofmann, G. Csányi, A. C. Ferrari, M. C. Payne, J. Robertson, *Phys. Rev. Lett.* **2005**, *95*, 036101.
[23] X.-L. Zhou, X.-Y. Zhu, J. M. White, *Surf. Sci.* **1988**, *193*, 387 – 416.
[24] R. Joshi, R. Schielholz, J. J. Schneider, P. Haridoss, *Z. Anorg. Allg. Chem.* **2008**, *634*, 911 – 915.
[25] G. Kresse, J. Furthmüller, *Phys. Rev. B* **1996**, *54*, 11169 – 11186.
[26] P. E. Blöchl, *Phys. Rev. B* **1994**, *50*, 17953 – 17979.
[27] Y. Zhang, W. Yang, *Phys. Rev. Lett.* **1998**, *80*, 890 – 890.
[28] K. M. Neyman, S. Schauermann, *Angew. Chem.* **2010**, *122*, 4851 – 4854; *Angew. Chem. Int. Ed.* **2010**, *49*, 4743 – 4746.
[29] I. V. Yudanov, A. V. Matveev, K. M. Neyman, N. Rösch, *J. Am. Chem. Soc.* **2008**, *130*, 9342 – 9352.
[30] S. Shetty, A. P. J. Jansen, R. A. van Santen, *J. Am. Chem. Soc.* **2009**, *131*, 12874 – 12875.

